Progress In Electromagnetics Research C, Vol. 10, 163–173, 2009

EFFECTS OF COUPLING COEFFICIENT ON STATIC PROPERTIES OF BISTABLE QWS-DFB SEMICONDUCTOR LASER AMPLIFIERS

M. Aleshams

Department of Electrical and Computer Engineering
Islamic Azad University
Fasa Branch, Fasa, Iran

Abstract—We previously analyzed the effects of trapezoidal tapered gratings on the dispersive bistable characteristics of a quarter wavelength phase-shifted distributed feedback semiconductor laser amplifier (QWS-DFB-SLA). In this paper, we analyze the effects of coupling coefficient on the static bistable characteristics of a QWS-DFB SLA with a tapered or a non-tapered grating. Simulation results show that any change in the coupling coefficient can change the characteristics such as the spectral range of low-threshold bistable switching and the on-off switching contrast.

1. INTRODUCTION

A distributed feedback semiconductor laser amplifier (DFB-SLA), which is biased below oscillation threshold, similar to a Fabry-Perot semiconductor laser amplifier (FP-SLA) shows a dispersive optical bistability (OB) behavior.

Researchers have utilized optical bistability in SLA's for optical logic and optical signal processing [1–4]. This is due to the fact that SLA's exhibit exceptional bistability characteristics such as low switching powers ($\sim\mu$W), fast switching speeds ($\sim$ ns), inherent optical gain, and wavelength compatibility with optical communication systems [5]. Meanwhile, a bistable DFB-SLA in comparison to a bistable FP-SLA, offers the advantage of controlling the input/output characteristics by tailoring the DFB transmission through some non-uniformities of its grating [6].

Corresponding author: M. Aleshams (m_aleshams@yahoo.com).

The first team to study of bistability in DFB-SLA's was H. Kawaguchi et al., followed by M. J. Adams et al. [7–9]. In all these works, the DFB laser amplifier had a uniform ideal grating structure and two important results were obtained. The first was that optical bistability was observed at input power levels of a few μw, and the second was that, as a consequence of the spectral asymmetry of the bistable DFB-SLA, the hysteresis loops on either side of the stop band exhibited different shapes. Static and dynamic properties of dispersive optical bistability in uniform-grating DFB semiconductor lasers were investigated both theoretically and experimentally in 1995. The results showed that the OB switching speed could be increased by increasing the bias level from below to above threshold [10]. In 1997, it was shown that by introducing some non-uniformities such as spatial phase shift and chirp, some bistable static performance, such as the switching-on threshold and ON-OFF switching ratio could be improved [11]. The principle of an all-optical flip-flop based on dispersive bistability in a uniform-grating DFB-SLA was described in 2001 [12]. Using a bistable DFB-SLA as a two-wavelength switch was described in 2006 [13]. By introducing tapering to the grating of a quarter wavelength phase-shifted DFB-SLA (QWS-DFB-SLA), we showed that this non-uniformity can widen the spectral range of low-threshold bistable switching and increase the on-off switching contrast [14]. Finally, in a most recent report, we proposed a procedure to analyze transient response of bistable DFB-SLA's. The results of the analysis demonstrated that among bistable DFB-SLA's with uniform, QWS, and tapered gratings, the latter has the best switching behavior [15].

On the other hand, one of the important parameters assumed constant in previous studies on optical bistabilty in DFB structures is the coupling coefficient, κ. Since this parameter is associated with the perturbed relative permittivity, then its numerical value depends on the shape, depth and period of the corrugation. In this paper, our aim is to study the effects of change in the coupling coefficient on the bistable characteristics of a tapered or a non-tapered QWS-DFB SLA under steady-state conditions.

The layout of the paper is as follows: In Sec. 2, we present the procedure used to calculate the coupling coefficient along the cavity of a DFB structure. Based on the coupled-mode and carrier rate equations, in Sec. 3, we present the theoretical model used for our numerical analysis. In Sec. 4, we show that how the unsaturated amplifier gain and the steady-state bistable characteristics of QWS-DFB-SLA's are affected by changing the coupling coefficient. Finally, we close the paper by conclusions, in Sec. 5.

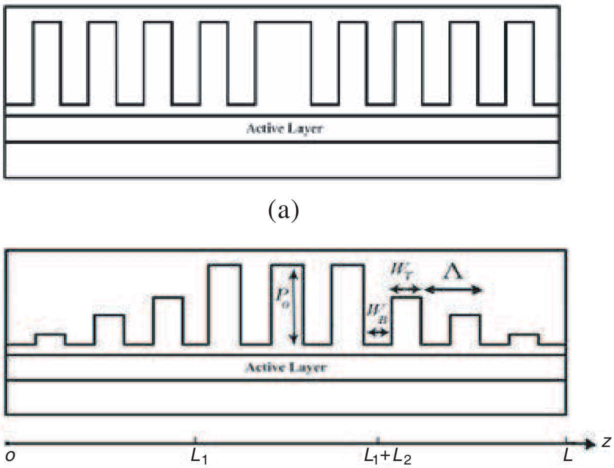

(a)

(b)

Figure 1. Schematic diagram of a DFB-SLA with: (a) Purely QWS, and (b) trapezoidal tapered purely QWS gratings.

2. THE COUPLING COEFFICIENT IN DFB STRUCTURE

Schematics of the various DFB gratings used in our analysis are shown in Fig. 1. Fig. 1(a) illustrates a purely QWS grating, while Fig. 1(b) shows a trapezoidal tapered QWS grating whose depth, p, is a function of the axial variable, z, as follows

$$p(z) = \begin{cases} p_0\left(1 - \frac{(L_1 - z)}{L_1}\right) & 0 < z \leq L_1 \\ p_0 & L_1 \leq z \leq L_1 + L_2 \\ p_0\left(1 - \frac{(z-(L_1+L_2))}{L-(L_1+L_2)}\right) & L_1 + L_2 \leq z < L \end{cases} \tag{1}$$

where P_0 is the maximum depth of the grating, W_B and W_T are width of the bottom and top corrugations, respectively, Λ is period of the grating, L_1 is the length of the left section with a tapered grating, L_2 is the length of the middle section with a uniform grating, and L the total length. It is obvious that the minimum grating depth which occurs at both ends of the DFB is greater than zero.

Ghafouri-Shiraz et al. [16] presented a procedure to calculate the coupling coefficient, κ for a uniform-grating sub-section of length l and we summarize this procedure in a flowchart illustrated in Fig. 2.

Based on this procedure, the numerical value of κ depends on the shape, depth and period of the corrugation, Λ and therefore, it is a

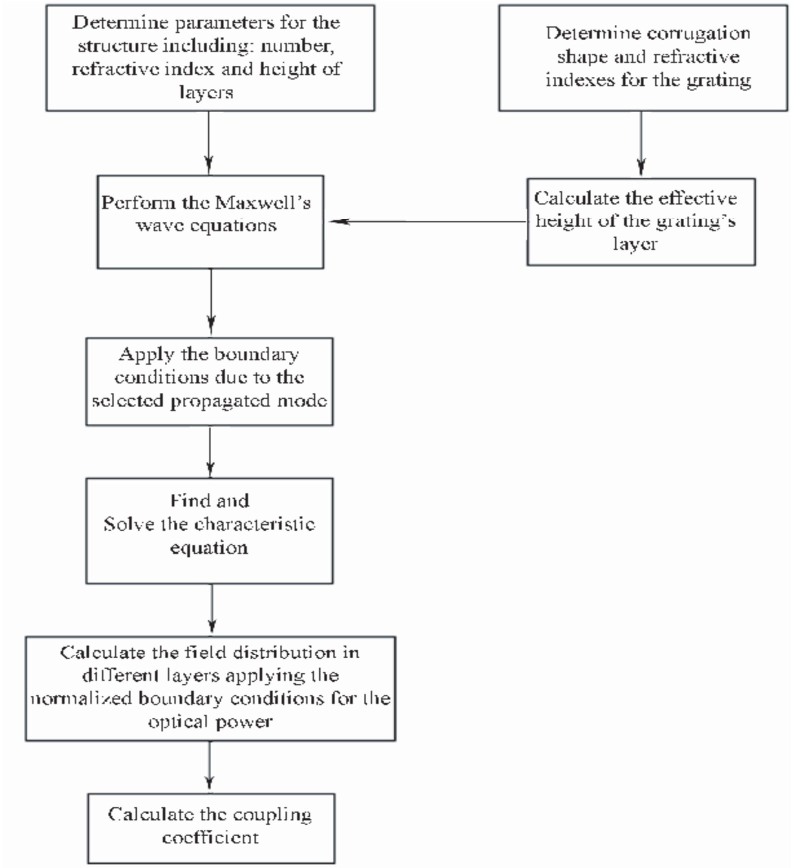

Figure 2. A flow chart to obtain the coupling coefficient for a uniform grating subsection of a DFB structure.

function of the axial variable for the tapered QWS-DFB structure. In comparison to the coupling coefficient obtained from a purely QWS-DFB laser, one need to calculate the $\kappa_{eff} \cdot L$ product for the tapered structure and compare it with $\kappa \cdot L$ product obtained for a non-tapered structure. Definition of the κ_{eff} for a non-uniform QWS-DFB structure is,

$$\kappa_{eff} = \frac{\int_0^L \kappa(z)\, dz}{L} \tag{2}$$

It is obvious that by changing a parameter such as the maximum depth of the grating, one can change the value of $\kappa_{eff} \cdot L$ in the tapered QWS-DFB SLA, or similarly the value of $\kappa \cdot L$ in the purely QWS-DFB SLA.

3. THEORETICAL MODEL

If $A(z)$ and $B(z)$ are the slowly varying amplitudes of the forward and backward propagating fields through the DFB structure, respectively, then the coupled-mode equations can be defined as [17]

$$\frac{dA}{dz} = i\Delta\beta A + i\kappa B \tag{3a}$$

$$\frac{dB}{dz} = -i\Delta\beta B - i\kappa A \tag{3b}$$

where $\Delta\beta = \beta - \beta_0$ is the detuning of the wave number β from the Bragg wave number, $\beta_0 = \pi/\Lambda$ and defined by

$$\Delta\beta = \delta - ig(1 - i\alpha)/2 + i\alpha_{int}/2 \tag{4}$$

where δ is due to the detuning of the free-space wavelength from the Bragg wavelength, α is the line width enhancement factor and governs the change in the refractive index through variations in the carrier density, α_{int} is the internal loss due to scattering and free carrier absorption, and g is the modal power gain given as

$$g = \Gamma a\,(N - N_0) \tag{5}$$

where Γ is the optical confinement factor, a is the differential gain parameter, N is the carrier density, and N_0 is the carrier density at transparency.

The rate equation for the carrier density, N in a semiconductor laser amplifier is given by

$$\frac{dN}{dt} = \frac{J}{ed} - \frac{N}{\tau_c} - \frac{g}{\hbar\omega_0} I \tag{6}$$

where J is the current density in the active region of thickness d, e is the electron charge, τ_c is the carrier life time. $\hbar\omega_0$ is the photon energy, and $I = |A(z)|^2 + |B(z)|^2$ is the optical intensity. The carrier density for CW signals and pulses much wider than the carrier life time τ_c (~ 100) ps reaches a steady state with the value

$$N = \frac{\bar{J} + \bar{I}}{1 + \bar{I}} N_0 \tag{7}$$

where $\bar{J} = J/J_0$ is the current density normalized to its value required to achieve transparency $J_0 = edN_0/\tau_c$ and $\bar{I} = I/I_{\text{sat}}$ is the optical intensity normalized to the saturation intensity $I_{\text{sat}} = \hbar\omega_0/\Gamma a\tau_c$. Substituting (7) into (5) results in a new expression for the modal power gain:

$$g = \frac{g_0}{1 + \bar{I}} \tag{8}$$

where $g_0 = \Gamma a N_0 (J/J_0 - 1)$ is the unsaturated value of the modal power gain.

For our analysis, as mentioned in [14], we use a transfer-matrix representation (TMM) of the propagation in the cavity of the QWS-DFB structures with the boundary conditions neglecting facets reflectivity's given by

$$\begin{aligned} A\,(z=0) &= A_i \\ B\,(z=0) &= A_r \\ B\,(z=L) &= 0 \\ A\,(z=L) &= A_t \end{aligned} \tag{9}$$

where A_i, A_r, and A_t are the slowly varying amplitudes of the incident, reflected, and transmitted optical waves, respectively.

4. NUMERICAL RESULTS

It has been demonstrated that in a DFB-SLA, the optical bistability exists for values of the normalized detuning, δL less than those corresponding to the transmission peaks, (i.e., at the cavity resonances) [11]. In order to determine the cavity resonance frequencies, for a QWS-DFB-SLA, we first study its transmission characteristics for an input optical signal of $I \ll I_{\text{sat}}$. In this situation, by neglecting in the denominator of (8), one can approximate $g \approx g_0$.

On the other hand, optical bistability occurs as the gain of a DFB-SLA is saturated by increasing its optical intensity within the device. The intensity profile in an active semiconductor will create a gain profile via saturation. The modal gain, however, is used in the calculation of the transfer-matrix elements, which are in turn used to compute the optical intensity distribution. To account for this nonlinear behavior, we solve for the gain and intensity distributions using an iterative approach [11].

By choosing $\kappa_{eff} \cdot L$ (or $\kappa \cdot L$) $= 3$, we previously calculated the wavelength dependence of the transmission gain $G = I_{out}/I_{in} = |A_t|^2/|A_i|^2$ and the bistability hysteresis for the mentioned QWS-DFB laser amplifiers which the results have been contributed in [14]. Now we explore how these results are affected if we change the coupling coefficient.

4.1. A Decrease in the Coupling Coefficient

By decreasing the coupling coefficient, the wavelength dependence of the transmission gain of the purely QWS-DFB-SLA is shown in Fig. 3(a). The parameter $g_0 L = 1.3527$ is chosen to realize $G = 30\,\text{dB}$

centered at the detuning $\delta L = 3.32$, where as shown in Fig. 3(b) the transmission peak can be achieved with $g_0 L = 2.032$ centered at the detuning $\delta L = 4.95$ for the tapered QWS-DFB laser amplifier.

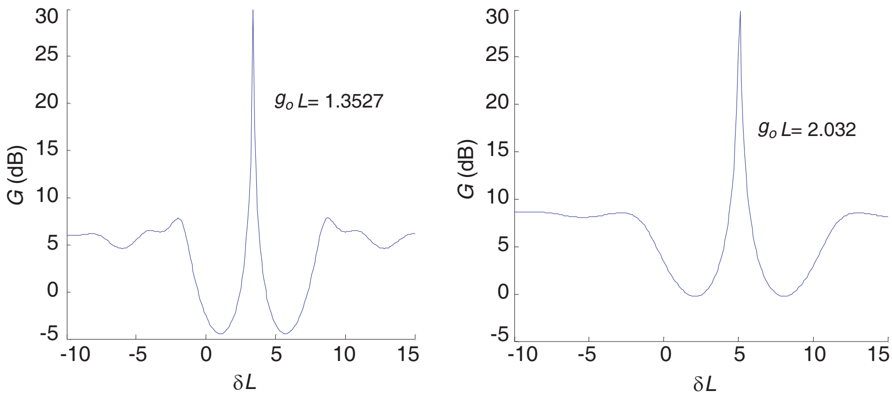

(a) (b)

Figure 3. Wavelength dependence of the amplifier gain, G, with $\alpha = 5$ and $\alpha_{int} = 0$ for: (a) The purely QWS-DFB SLA with $\kappa L = 2$ and $g_0 L = 1.3527$ corresponding to $G = 30\,\text{dB}$; (b) The trapezoidal tapered QWS-DFB SLA with $\kappa_{eff} L = 2$ and $g_0 L = 2.032$ corresponding to $G = 30\,\text{dB}$.

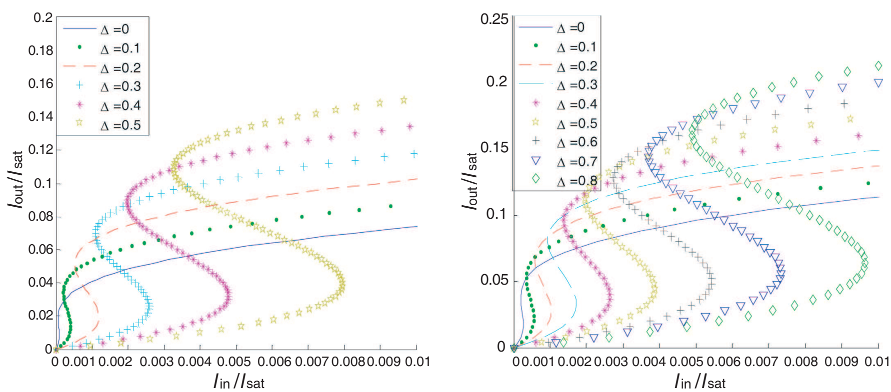

(a) (b)

Figure 4. The bistability characteristics with $\alpha = 5$, $\alpha_{int} = 0$, and $\Delta = \delta L' - \delta L$ as a parameter for: The purely QWS-DFB SLA with $\kappa L = 2$ and $g_0 L = 1.3257$ corresponding to $G = 30\,\text{dB}$; (b) The trapezoidal tapered QWS-DFB SLA with $\kappa_{eff} L = 2$, $g_0 L = 2.032$ corresponding to $G = 30\,\text{dB}$.

We can plot the bistability hysteresis for the QWS-DFB laser amplifiers with the values for δL less than that corresponding to the transmission peak. As shown in Fig. 4(a), starting from a value of δL near the onset of bistability (i.e., $\delta L' = 3.25$), by decreasing δL the bistable region of input intensities will increase for the purely QWS-DFB SLA. Meanwhile, the value of $g_0 L$ is selected to yield an unsaturated peak $G = 30\,\text{dB}$ for the DFB laser amplifier. On the other hand, the bistability hysteresis for the tapered QWS-DFB is demonstrated in Fig. 4(b), the highest value of the δL ($\delta L' = 4.75$) is selected to be near the onset of bistability and then it is decreased until the switch-on input intensity reached 1% of the saturation intensity. As illustrated in Fig. 4, the detuning range for the low-threshold bistable switching for the QWS-DFB amplifiers is wider than that calculated in [14]. The hysteresis is also increased in contrast by decreasing the coupling coefficient for both of the tapered and non-tapered cases. However, the top level of bistability characteristics is not flat as that calculated in [14] for the two QWS-DFB SLA's.

4.2. An Increase in the Coupling Coefficient

Now we increase the coupling coefficient rather the value selected in [14]. The wavelength dependence of the transmission gain of the purely QWS-DFB-SLA is shown in Fig. 5(a). The parameter

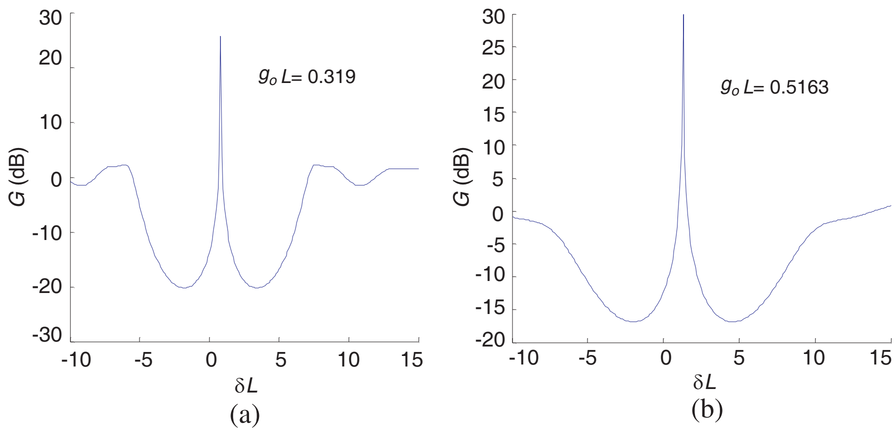

Figure 5. Wavelength dependence of the amplifier gain, G, with $\alpha = 5$ and $\alpha_{int} = 0$ for: The purely QWS-DFB SLA with $\kappa L = 4$ and $g_0 L = 0.319$ corresponding to $G = 30\,\text{dB}$; (b) The trapezoidal tapered QWS-DFB SLA with $\kappa_{eff} L = 4$ and $g_0 L = 0.5163$ corresponding to $G = 30\,\text{dB}$.

$g_0L = 0.319$ is chosen to realize $G = 30\,\text{dB}$ centered at the detuning $\delta L = 0.78$, where as shown in Fig. 5(b) the transmission peak can be achieved with $g_0L = 0.5163$ centered at the detuning $\delta L = 1.65$ for the tapered QWS-DFB laser amplifier.

The bistability hysteresis for the QWS-DFB laser amplifiers are shown in Fig. 6. As shown in Fig. 6(a), the highest value of the δL (i.e., $\delta L' = 0.713$) is selected to be near the onset of bistability for the purely QWS-DFB SLA and then it is decreased until the switch-on input intensity reached 1% of the saturation intensity. On the other hand, the bistability hysteresis for the tapered QWS-DFB is demonstrated in Fig. 6(b), the highest value of the δL ($\delta L' = 1.1671$) is chosen to be near the onset of bistability. Meanwhile, the value of g_0L is selected to yield an unsaturated peak $G = 30\,\text{dB}$ for the DFB laser amplifier. As illustrated in Fig. 6, the detuning range of approximately for the low-threshold bistable switching for the QWS-DFB amplifiers is narrower than that calculated in [14]. The hysteresis is also decreased in contrast by increasing the coupling coefficient for both of the tapered and non-tapered cases. However, the top level of bistability characteristics is flatter than as that calculated in [14] for the two QWS-DFB SLA's.

4.3. Analysis of the Results

In fact, when we decrease or increase the coupling coefficient of a QWS-DFB amplifier, it seems that feedback for the wavelength

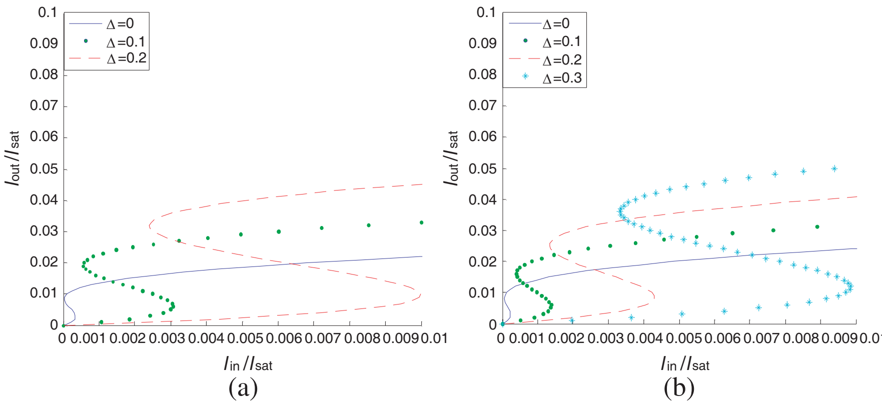

(a) (b)

Figure 6. The bistability characteristics with $\alpha = 5$, $\alpha_{int} = 0$, and $\Delta = \delta L - \delta L$ as a parameter for: The purely QWS-DFB SLA with $\kappa L = 4$ and $g_0L = 0.319$ corresponding to $G = 30\,\text{dB}$; (b) The trapezoidal tapered QWS-DFB SLA with $\kappa_{eff}L = 4$, $g_0L = 0.5163$ corresponding to $G = 30\,\text{dB}$.

corresponding to the Bragg wave number is decreased or increased, respectively. This decrease or increase requires the SLA's to be pumped at a higher or a lower modal gain (g_0), respectively rather than those given in [14] to achieve the same unsaturated peak amplifier gain (G). Moreover, due to the nonzero line width enhancement factor, an increase or a decrease in the modal gain results in a decrease or an increase in the refractive index, respectively and so a decrease or an increase in the cavity resonance wavelength. Consequently, the transmission spectrum shifts to higher or lower values of δ, respectively.

On the other hand, an increase or a decrease in modal gains increases or decreases the switching contrast, respectively. Moreover, a wider or a lower range of wavelengths exhibit low-threshold switching because the increased or decreased gain strengthens or weakens the intensities, respectively at these wavelengths.

5. CONCLUSION

In this paper, by calculating the steady-state bistable response of the QWS-DFB laser amplifiers, we have shown that the spectral range and also the contrast of the low-threshold bistable switching can be affected if we change the coupling coefficient. Although a decrease in the coupling coefficient shows improvements in these bistability characteristics which are useful for several applications in optical communication systems [1–3], the slope of the top level of the bistable hysteresis increases. Therefore, it may have fewer applications in bistability-based optical signal regenerators [4], which produce pulses with flatter peaks.

REFERENCES

1. Inoue, K., "All-optical flip-flop operation in an optical bistable device using two lights of different frequencies," *J. Op. Lett.*, Vol. 12, 918–920, 1987.
2. Sharfin, W. F. and M. Dagenais, "High contrast, 1.3 mm optical and gate with gain," *J. Appl. Phys. Lett.*, Vol. 48, 321–322, 1986.
3. Sharfin, W. F. and M. Dagenais, "Femtojoule optical switching in nonlinear semiconductor laser amplifiers," *J. Appl. Phys. Lett.*, Vol. 48, 1510–1512, 1986.
4. Webb, R. P., "Error-rate measurements on an all-optically regenerated signal," *J. Opt. Quantum*, Vol. 19, 57–60, 1987.
5. Adams, M. J., H. J. O. Westlake, and M. J. Mahony, "Optical bistability in semiconductor laser amplifiers," *Optical*

Nonlinearities and Instabilities in Semiconductors, H. Haug (ed.), Academic Press, San Diego, 1988.

6. Winfull, H. G., J. H. Marburger, and E. Garmire, "Theory of bistability in nonlinear distributed feedback structures," *J. Appl. Phys. Lett.*, Vol. 35, 379–381, 1979.
7. Kawaguchi, H., K. Inoue, T. Matsuoka, and K. Otsuka, "Bistable output characteristics in semiconductor laser injection locking," *IEEE J. of Quantum Electron.*, Vol. 21, 1314–1317, 1985.
8. Adams, M. J. and R. J. Wyatt, "Optical bistability in distributed feedback semiconductor laser amplifiers," *Proc. Inst. Elect. Eng.*, Vol. 134, 35–40, 1987.
9. Magari, K., H. Kawaguchi, M. Fukuda, and K. Oe, "Optical narrow-band filters using optical amplification with distributed feedback," *IEEE J. Quantum Electron.*, Vol. 24, 2178–2190, 1988.
10. Hui, R., "Static and dynamic properties of dispersive optical bistability in semiconductor lasers," *J. Lightwave Technology*, Vol. 13, 42–48, 1995.
11. Maywar, D. N. M. and G. P. Agrawal, "Transfer-matrix analysis of optical bistability in DFB semiconductor laser amplifiers with nonuniform gratings," *IEEE J. Quantum Electron.*, Vol. 33, 2029–2037, 1997.
12. Maywar, D. N. M. and G. P. Agrawal, "All-optical hysteresis control by means of cross-phase modulation in semiconductor optical amplifiers," *J. Opt. Soc. Amer.*, Vol. 18, 1003–1013, 2001.
13. Hurtado, A., "Two-wavelength switching with a distributed feedback semiconductor optical amplifier," *IEE Proc. Optoelectronics*, Vol. 153, 21–27, 2006.
14. Aleshams, M., M. K. Moravvej-Farshi, and M. H. Sheikhi, "Tapered grating effects on static properties of a bistable QWS-DFB semiconductor laser amplifier," *Solid State Electron.*, Vol. 52, 156–163, 2008.
15. Aleshams, M., M. K. Moravvej-Farshi, and M. H. Sheikhi, "Switching behavior of bistable DFB Semiconductor laser amplifiers," *Fiber and Integrated Optics*, Vol. 28, 275–287, 2009.
16. Ghafouri-Shiraz, H. and B. S. K. Lo, *Distributed Feedback Laser Diodes: Principles and Physical Modeling*, John Wiley & Sons, 1996.
17. Agrawal, G. P. and N. K. Dutta, *Semiconductor Lasers*, Van Nostrand Reinhold, New York, 1993.